The EMBO Journal Vol. 21 No. 6 pp. 1280–1288, 2002

The cell morphogenesis gene *ANGUSTIFOLIA* encodes a CtBP/BARS-like protein and is involved in the control of the microtubule cytoskeleton

U.Folkers, V.Kirik[1], U.Schöbinger, S.Falk[1], S.Krishnakumar[2], M.A.Pollock[2], D.G.Oppenheimer[2], I.Day[3], A.R.Reddy[3], G.Jürgens and M.Hülskamp[1,4]

ZMBP, Entwicklungsgenetik, Universität Tübingen, Auf der Morgenstelle 1, D-72076 Tübingen, [1]University of Köln, Botanical Institute III, Gyrhofstrasse 15, D-50931 Köln, Germany, [2]Department of Biological Sciences, University of Alabama, 301 Biology, Tuscaloosa, AL 35487-0344 and [3]Department of Biology, Colorado State University, Fort Collins, CO 80526, USA

[4]Corresponding author
e-mail: martin.huelskamp@uni-koeln.de

The *ANGUSTIFOLIA* (*AN*) gene is required for leaf hair (trichome) branching and is also involved in polarized expansion underlying organ shape. Here we show that the *AN* gene encodes a C-terminal binding proteins/brefeldin A ADP-ribosylated substrates (CtBP/BARS) related protein. *AN* is expressed at low levels in all organs and the AN protein is localized in the cytoplasm. In *an* mutant trichomes, the organization of the actin cytoskeleton is normal but the distribution of microtubules is aberrant. A role of *AN* in the control of the microtubule cytoskeleton is further supported by the finding that *AN* genetically and physically interacts with *ZWICHEL*, a kinesin motor molecule involved in trichome branching. Our data suggest that CtBP/BARS-like protein function in plants is directly associated with the microtubule cytoskeleton.

Keywords: *Angustifolia*/*Arabidopsis*/cell morphogenesis/microtubules/trichomes

Introduction

The particular shape that plant cells adopt not only relates to their function but also affects the overall shape of plant organs. Because of this inter-relationship between plant cell shape and organ shape, it is important to understand how cell shape is regulated. *Arabidopsis thaliana* is an excellent model to study this problem. Mutations in the *ANGUSTIFOLIA* (*AN*) gene affect the morphogenesis of some cell types specifically, such as leaf hairs (trichomes), as well as the shape of various organs, such that cotyledons and the rosette leaves are narrow, and the seed pods (siliques) are twisted (Redei, 1962; Hülskamp *et al*., 1994; Tsukaya *et al*., 1994; Tsuge *et al*., 1996).

The control of organ shape is best studied in leaves. Several mutants affect leaf morphology. Whereas one class of mutants shows general defects in cell expansion, e.g. dwarf mutants, a different class of mutants is defective in polarized cell expansion, resulting in leaves that are narrower or wider than the wild type. In particular, the latter class is instructive for an understanding of the spatial regulation of cell form. Three mutants, *rotundifolia 1*, (*rot1*), *rot2* and *rot3*, have cells that are widened at the expense of cell length, such that leaves are short and wide without changes in cell number (Tsukaya, 1995; Tsuge *et al*., 1996). Mutations in the *AN* gene result in the opposite phenotype: leaves that are narrower and thicker than normal, but longer (Tsukaya, 1995; Tsuge *et al*., 1996). A detailed morphological study of both cotyledons and rosette leaves on *an* mutants has shown that the narrow organ phenotype is due to a defect in polarized cell expansion. Cells are generally smaller in the leaf-width direction and larger in the leaf-thickness direction. The *an rot* double mutant showed an additive phenotype, which indicated that the two processes are regulated by independent pathways (Tsukaya, 1995; Tsuge *et al*., 1996).

Trichomes represent a well-studied model system for the spatial regulation of morphogenesis at the single-cell level (Marks, 1997; Oppenheimer, 1998; Hülskamp *et al*., 1999). One major advantage is that trichomes have a distinct structure and polarity. Trichomes originate from single epidermal cells that stop dividing and start to endoreduplicate. After three or four endoreduplication cycles, trichome cells undergo two successive branching events. The mature trichome is a three-branched, 500-μm-tall, single cell. The branching pattern provides excellent criteria by which to identify specific mutations that affect cell morphogenesis. More than 15 branching mutants have been isolated to date in which branch number is altered. Two classes of trichome branching mutants can be distinguished. The first class comprises trichome branch number mutants that also have an altered DNA content. An increased DNA content has been correlated with an increase in branch number, and trichomes with a reduced DNA content have fewer branches than the wild type (Koornneef *et al*., 1982; Hülskamp *et al*., 1994; Perazza *et al*., 1999). Because cellular DNA content is also correlated with cell size, it has been hypothesized that trichome branch number is controlled by cell size or cell growth. The second class consists of branch number mutants that have a normal DNA content. This class includes eight mutants that have a reduced branch number (Hülskamp *et al*., 1994; Folkers *et al*., 1997; Krishnakumar and Oppenheimer, 1999; Luo and Oppenheimer, 1999) and one mutant that has an increased branch number (Folkers *et al*., 1997). A detailed genetic analysis of these mutants has revealed that most double mutant combinations show an additive phenotype, suggesting that the genes act in independent pathways (Oppenheimer, 1998; Hülskamp, 2000). Double mutant combinations of underbranched mutants and the overbranched *noeck* (*nok*) mutant yielded intermediate phenotypes in most cases. Only the two-branched mutants *an*

and *furca 4* (*frc4*) were epistatic to *nok*, suggesting that only *AN* and *FRC4* are controlled by *NOK* (Folkers *et al*., 1997; Luo and Oppenheimer, 1999).

Little is known about the cellular and biochemical processes underlying cell morphogenesis. However, the microtubule cytoskeleton appears to be important for establishing and maintaining cell polarity. One line of evidence comes from the analysis of two mutants displaying a reduced branching phenotype. The *ZWICHEL* (*ZWI*) gene encodes a kinesin motor protein with a calmodulin-binding domain. This strongly suggests that microtubule-based transport is important for branch formation (Reddy *et al*., 1996b; Oppenheimer *et al*., 1997). In *fass* (*fs*) mutants, cell shape changes are correlated with an aberrant microtubule cytoskeleton, and it is therefore conceivable that the unbranched trichome phenotype in *fs* mutants is also caused by defects in microtubule organization (Torres-Ruiz and Jürgens, 1994; Traas *et al*., 1995). Recent drug inhibitor studies support this interpretation. The application of drugs that disrupt the microtubule cytoskeleton results in a loss of trichome polarity, leading to bloated trichome cells with a reduced branch number (Szymanski *et al*., 1999; Mathur and Chua, 2000).

To analyze the molecular mechanisms underlying cell morphogenesis, we have isolated the *AN* gene. We show that *AN* encodes a C-terminal binding proteins/brefeldin A ADP-ribosylated substrates (CtBP/BARS)-like protein and provide evidence that *AN* is involved in the regulation of the microtubule cytoskeleton.

Results

Positional cloning of the AN gene

We isolated the *AN* gene by a positional cloning approach. Initially, the *AN* gene was mapped between the molecular marker nga59 and the *ECERIFERUM 1* (*CER1*) gene on chromosome I. For further fine mapping, recombination breakpoints between *AN* and *CER1* were mapped in ~10 000 meiotic events from a cross between the *an–cer1* double mutant (Landsberg *erecta*; L*er*) and a wild-type (Niederzenz; Nd) plant. Recombinants were identified in the F_2 generation as *an* mutant plants not displaying the *cer1* phenotype. In ~2000 F_1 events from the same cross, recombinant breakpoints between *AN* and nga59 were mapped using molecular markers (Figure 1A). A YAC and BAC/P1 contig was established between *CER1* and nga59. Several new CAPS markers were developed, and the *AN* gene was localized to a 20 kb interval that comprises seven potential genes (for details see Figure 1A). To identify the *AN* gene, we sequenced genomic DNA from wild-type and *an* alleles for several of the candidate genes. Allele-specific polymorphisms were found in a gene annotated as a dehydrogenase (Figure 1B; Table I). All ethylmethanesulfonate (EMS) induced alleles, except *an-EM1*, displayed a G to A transition leading to a stop codon or defects in splice acceptor sites. The two X-ray-induced mutants, *an-X1* and *an-X2*, have a single base deletion and an inversion, respectively (Table I).

To determine the genomic structure of the *AN* gene, cDNA fragments were amplified from total RNA of young rosette leaves by RT–PCR. Sequencing of the amplified cDNA fragments revealed a 1908 bp open reading frame (ORF). Our sequences matched the cDNA clone deposited in DDBJ/EMBL/GenBank with accession No. AB032060. The comparison with the genomic sequence revealed seven exons and six introns. The transcription start site is predicted to be 37 bp downstream of the TATA box. Upstream of the *AN* coding sequence, a short ORF was found. The stop codon of the short ORF overlaps with the predicted start codon of the *AN* gene.

A 4 kb genomic fragment containing the *AN* coding region and the complete non-coding region between the two flanking genes was used to complement the *an* mutant. The majority of the 24 transformants showed only partial rescue of the *an* trichome phenotype, suggesting that additional regulatory sequences are needed for full expression of the *AN* gene.

Sequence comparisons of the AN protein

The *AN* gene is predicted to encode a protein of 636 amino acids. The AN protein sequence shows similarity to proteins and motifs in DDBJ/EMBL/GenBank (Figure 1B). The presence of the nuclear targeting sequence KKRH at position 424–427 suggests that the AN protein is nuclear localized. At position 328–361, a PEST motive was found in close proximity to a cell cycle-specific phosphorylation site (position 453–456). This suggests that AN protein is subject to cell cycle-dependent protein degradation.

The N-terminus of the AN protein shares sequence similarity with three protein classes, which also show similarities with each other in this region: dehydrogenases, CtBPs and BARS (Figure 2).

Sequence similarities were found to bacterial D-2-hydroxy acid dehydrogenases that catalyze the NADH-dependent reduction of 2-oxocarboxyl acids to their corresponding 2-hydroxycarboxyl acids. However, several amino acids, H296, D259 and E264, known to be important for the catalytic function in D-lactate-dehydrogenase (Asryants *et al*., 1989; Stoll *et al*., 1996; Bernard *et al*., 1997), are not present in AN, rendering it unlikely that AN functions as a dehydrogenase.

Sequence similarity of AN to CtBPs and BARS is less pronounced than between CtBPs and BARS themselves. Although CtBPs and BARS were initially identified by their different functions as transcriptional co-repressors (Nibu *et al*., 1998; Schaeper *et al*., 1998) and proteins involved in the regulation of Golgi dynamics, respectively (Matteis *et al*., 1994; Spanfo *et al*., 1999), the recent findings that CtBPs can function as BARS, and vice versa (Spanfo *et al*., 1999), suggests that they are homologs with a dual function.

The AN gene is evolutionarily conserved in plants

Database searches revealed putative *AN* homologs in various plant species (Figure 3). Expressed sequence tag (EST)-derived amino acid sequences with high sequence identity to the N-terminal region of the AN protein were found in *Glycine max*, *Lotus japonicus*, *Solanum tuberosum* and *Medicago truncatula*, and for the middle region, in *G.max*, *Triticum monococcum* and *M.truncatula*. Although the EST sequence comparisons were limited to small regions, the high percentage of amino acid sequence identities found in plants, but not in other species, suggests that these genes represent true *AN* orthologs.

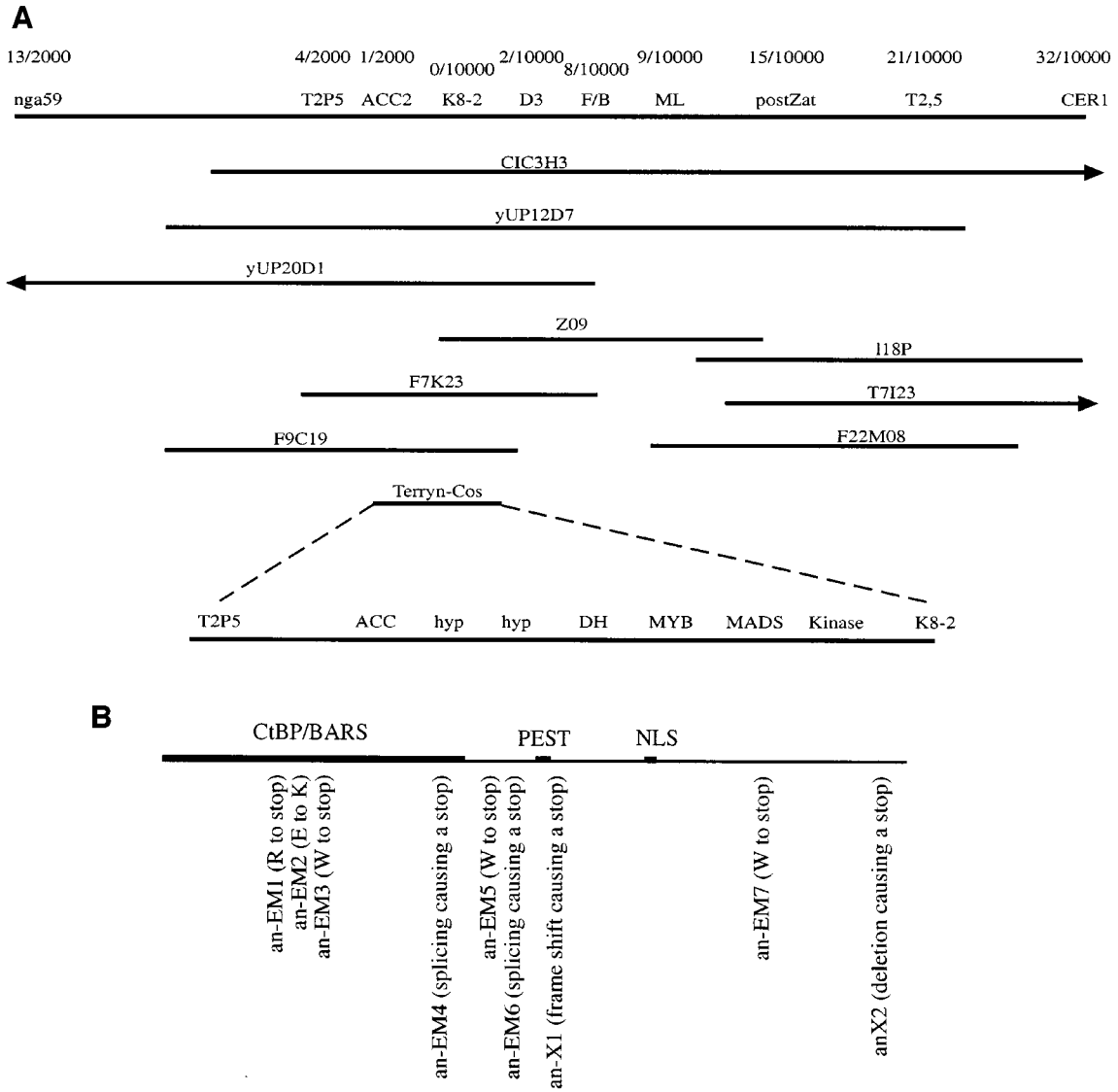

Fig. 1. Positional cloning and structure of the *AN* gene. (**A**) Relative position of the YACs, BACs and P1 clones in the nga59 CER1 interval. Clones marked with an arrowhead extend the interval shown in the figure. The molecular markers used for fine mapping and the number of recombinants are shown at the top. At the bottom, the Terryn-Cosmid is shown with the *AN* gene candidates left after fine mapping. hyp, hypothetical protein; DH, dehydrogenase; MYB, MYB-like transcription factor; MADS, MADS-box containing protein. (**B**) The relative position of putative protein domains is indicated at the top. The positions of mutations in different *an* alleles are shown below.

Expression analysis of AN

The pleiotropic phenotype of *an* mutants, affecting virtually all organs, suggests that *AN* is ubiquitously expressed. Attempts to study *AN* expression by northern blot hybridization revealed no signal, suggesting that *AN* is expressed either at very low levels or only in few cells. Using RT–PCR, we found *AN* expression in all tissues analyzed, including roots, leaves, stems and flowers (Figure 4).

In order to test whether AN regulates morphogenesis in a concentration-dependent manner, we created plants expressing the cDNA under the control of the cauliflower 35S promotor. This construct rescues the *an* mutant phenotype; however, it does not result in a new phenotype in a wild-type background. Leaf form and trichome branching were indistinguishable from the wild type (data not shown).

Intracellular localization of AN

The sequence similarity to the transcriptional co-repressor CtBP and the presence of a nuclear localization sequence motif suggest that the AN protein might be targeted to the nucleus. In order to test this, we constructed a fusion construct with green fluorescent protein (GFP) under the control of the 35S promotor from the cauliflower mosaic virus. The intracellular localization of this fusion construct was studied in onion cells in a transient assay. The AN–GFP fusion protein was found ubiquitously in the cytoplasm and the nucleus (Figure 5A). No enrichment in specific subcellular compartments was found.

Analysis of the cytoskeleton in an mutants

As the sequence similarities of AN to other proteins do not immediately suggest in what cellular processes it might be involved, we assessed its role in the organization of the

Table I. Molecular analysis of *angustifolia* alleles

Allele	Mutation	Position (cDNA)	Protein	Position
an-EM1	C to T	343	R to stop	115
an-EM2	G to A	351	E to K	118
an-EM3	G to A	439	W to stop	147
an-EM4	G to A	754/755	splicing	252
an-EM5	G to A	871	W to stop	291
an-EM6	G to A	884/885	splicing	295
an-EM7	G to A	1603	W to stop	525
an-X1	one base deletion	725	frame shift	342
an-X2	4 kb inversion leading to a 26 bp and 3′ UTR deletion	1884	deletion of 8 AA	628

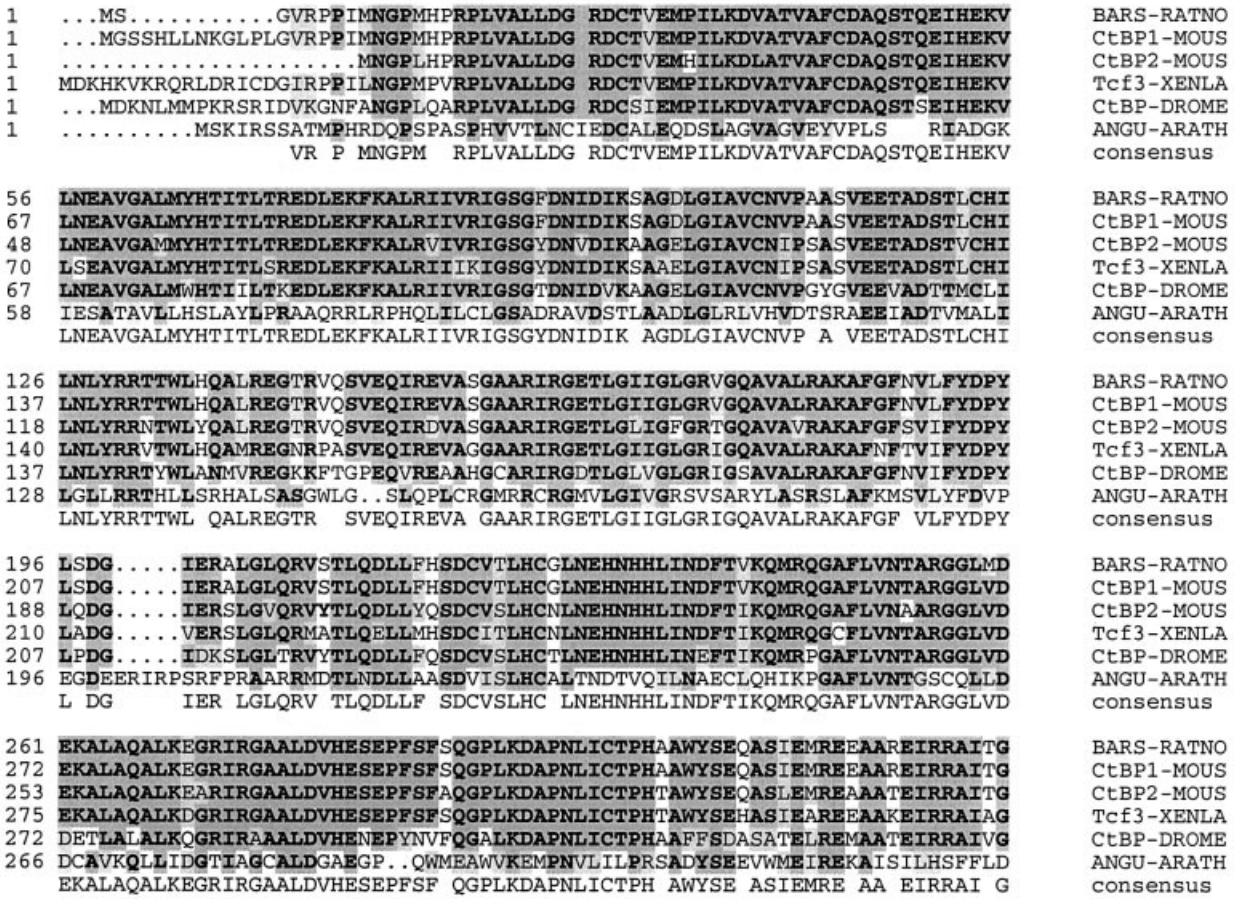

Fig. 2. Sequence comparison between AN and CtBP/BARS from other organisms. Identical amino acids are marked in bold on a dark gray background and similar amino acids are printed on a light gray background. MOUS, *Mus musculus*; RATNO, *Rattus norvegicus*; Tcf3-XENLA, T-cell factor 3 from *Xenopus laevis*; DROME, *Drosophila melanogaster*; ANGU-ARATH, AN from *A.thaliana.*

cytoskeleton, one of the major components controlling cell architecture.

The actin cytoskeleton was studied in *an* mutant plants expressing GFP–talin under the control of the 35S promotor (Mathur *et al*., 1999). The organization of the actin cytoskeleton, as visualized by the talin-mediated localization of GFP, was indistinguishable from the wild type (data not shown).

The microtubules were visualized by a GFP–MAP4 fusion protein that was expressed under the control of the trichome-specific GL2 promotor (Figure 5B–E). In a wild-type background, microtubules exhibited rapid changes during development. In incipient trichomes and all stages until branch initiation is completed, cortical microtubules are organized barrel like. During these stages, microtubule density is much higher in the tip region than at the base of the trichome. After branch formation, the cortical microtubules reorientate and become orientated longitudinally (Mathur and Chua, 2000). In *an* mutants, the orientation of microtubules was similar to that in the wild type. A striking difference, however, was found for the relative microtubule densities within the cell. While wild-type

Fig. 3. AN homologs in other plant species. A comparison of the AN amino acid sequence revealed conserved regions in ESTs of other plant species. (**A**) ESTs depicting sequence similarity in the mid-region of the AN protein. (**B**) ESTs depicting sequence similarity with the 3′ region of the AN protein. Lotus, *L.japonicus* (DDBJ/EMBL/GenBank accession No. AV408242); potato, *S.tuberosum* (accession No. BG589819); soybean, *G.max* (accession No. AW597150, BE020800); medicago, *M.truncatula* (accession No. AW690917, AW587381); wheat, *T.monococcum* (accession No. BF200009).

trichomes showed an increased microtubule density in the tip regions during all stages before and at branch formation, microtubule density in *an* mutants was not changed along the basal–apical axis. This visual impression was confirmed by determining the apical–basal ratios of microtubule density in wild-type and *an* mutant trichomes. In the wild type, the ratio was 4/1 (n = 18) and in *an* mutants it was 1.2/1 (n = 26). Thus, in the wild type, microtubule density is ~4 times higher in the tip region as compared with the basal region, whereas in *an* mutants no significant accumulation was found.

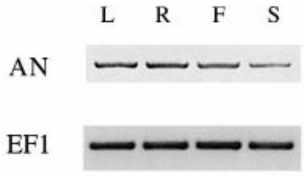

Fig. 4. Expression analysis and intracellular localization of AN. RT–PCR expression analysis of *AN* in different organs. The expression of EF1 was used as a control. L, leaf; R, root; F, flowers; S, stem.

Genetic and molecular interaction of AN and ZWI

To assess further the potential role of *AN* in the regulation of the microtubule cytoskeleton, we concentrated on its relationship with the *ZWI* gene, which encodes a kinesin-like motor molecule and provides a natural link to the involvement of AN in the control of microtubule organization or function (Reddy *et al*., 1996a,b; Oppenheimer *et al*., 1997; Song *et al*., 1997).

A genetic interaction between *AN* and *ZWI* was shown by the finding that double-heterozygous plants of certain *zwi* and *an* allele combinations exhibit more branches than the corresponding wild types. In F_1 plants from a cross between *zwi-w2* and *an-EM6*, up to four branch points were observed. This effect was allele specific because combinations of these two alleles with other *an* or *zwi* alleles did not show extra branch formation (Table II). In *an-EM6* mutants, a G to A transition in the splice/acceptor site of the third intron is likely to reduce the efficiency of correct splicing. Sequence analysis of the *zwi-w2* allele revealed a C to T transition that results in a stop codon at amino acid position 72. However, there is an in-frame AUG ~20 bp downstream from this stop codon, so we hypothesize that re-initiation of translation may occur.

Because this type of genetic interaction often indicates that the products of the two genes physically interact, we tested the hypothesis that AN and ZWI/KCBP physically interact by using the yeast two-hybrid system (Durfee *et al*., 1993). The N-terminal portion of *ZWI/KCBP* (not including the motor or calmodulin-binding domains) was cloned into pAS1CYH2 as a fusion to the GAL4 binding domain (Nt*KCBP*/pAS1CYH2). The *AN* gene was cloned into pACT2 as a fusion to the activating domain. Yeast containing the Nt*KCBP*/pAS1CYH2 plasmid were transformed with AN/pACT2. Transformants grew on media without leucine and tryptophan (–L/–W) but not on media without leucine, tryptophan and histidine (–L/–W/–H), and the colonies from the –L/–W plates showed no

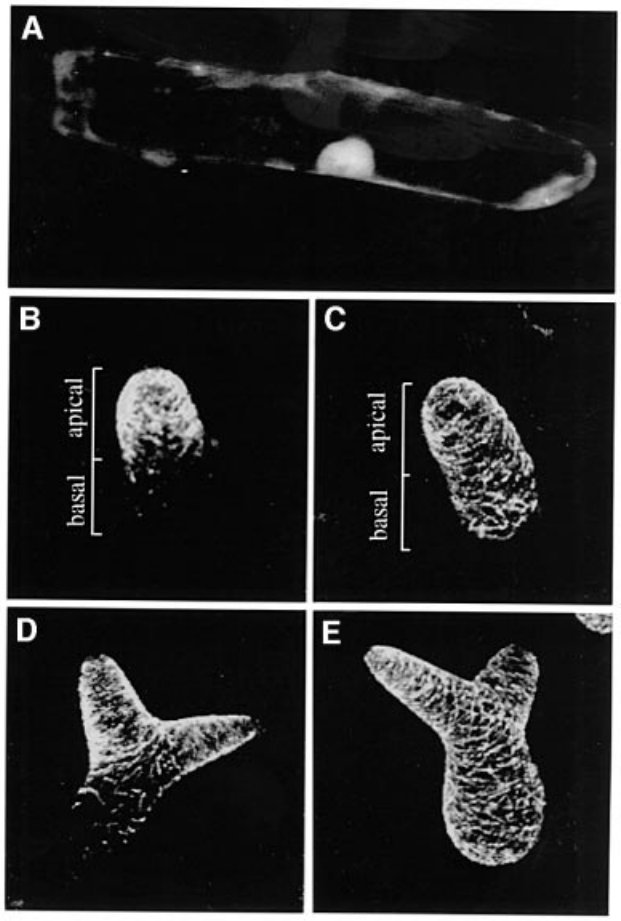

Fig. 5. Intracellular localization of AN and comparison of the microtubule organization. (**A**) Intracellular localization of GFP–AN in onion cells. Microtubule organization in trichomes using the GL2–GFP4–MAP4 line. (**B** and **D**) Wild type. (**C** and **E**) *an* mutant. (B and C) An incipient trichome shortly after growing out of the leaf surface. While wild-type trichomes show a denser network in the tip region, *an* mutants show an even distribution. (D and E) An elongated young trichome before branch initiation. Note that only the wild type has a denser microtubule network in the tip region.

β-galactosidase activity. However, when full-length *KCBP* was cloned into the pAS1CYH2 plasmid, and yeast was double-transformed with this plasmid and *AN*/pACT2, colonies grew on –L/–W/–H plates and showed β-galactosidase activity (see Figure 6, top).

Two other proteins that are known to interact with kinesin-like calmodulin-binding protein (KCBP) in yeast two-hybrid assays were also tested for their interaction with AN to determine whether they also interact with it. KCBP-interacting protein kinase (KIPK) is a protein kinase that interacts with N-terminal and full-length KCBP (Day *et al*., 2000). KIPK was isolated as a pACT2 clone, and two subdomains, one containing the N-terminal non-catalytic domain (Sub 1) and one containing the C-terminal protein kinase catalytic domain (Sub 2), were also cloned into pACT2. The *AN* gene was cloned into pAS1CYH2 plasmid. Yeast two-hybrid assays were performed with the *KIPK* full-length and Sub 1, Sub 2 pACT2 plasmids. In addition, the *AN* gene was also used in an assay with a putative calcium-binding protein (M6), which was found in a screen with the motor domain of *KCBP* (T.R.Thomas, A.R.Reddy and I.Day, unpublished results) and with the motor domain of *KCBP* in pACT2. Colonies containing the *AN* gene together with each of these genes grew on –L/–W plates, indicating the presence of pACT and pAS plasmids. However, these colonies did not grow on –L/–W/–H plates. The colonies grown on –L/–W plates showed no β-galactosidase activity (see Figure 6, bottom).

Discussion

The *an* mutant is one of the few examples in which the altered morphogenesis of whole organs can be explained by specific polarity defects at the level of the single cells. This, in combination with the specific branching phenotype of trichomes, makes the *AN* gene a very valuable tool to study cell morphogenesis. What have we learned from the molecular characterization of the *AN* gene?

The AN gene encodes a CtBP/BARS-like protein

We cloned the *AN* gene by a positional approach. The presence of allele-specific polymorphisms in nine *an* alleles and the rescue of the *an* mutant phenotype with the genomic fragment prove the identity of the *AN* gene.

The deduced AN protein shows overall low-level sequence similarity to the transcriptional co-repressor CtBP and to BARS proteins (Nibu *et al*., 1998; Spanfo *et al*., 1999). The CtBPs were initially identified as co-repressors of the zinc-finger transcriptional repressors Krüppel, Knirps and Snail in *Drosophila* (Nibu *et al*., 1998). CtBPs bind to a seven amino acid-long consensus sequence at the C-terminus of these transcription factors. BARS were identified as proteins that become ADP ribosylated upon brefeldin A treatment in rats (Matteis *et al*., 1994). Brefeldin A is a fungal toxin that results in the transformation of Golgi stacks into a tubular–reticular network (Lippincott-Schwartz *et al*., 1989). Among others, one important aspect of the regulation of Golgi dynamics affected is the ADP ribosylation status of BARS (Matteis *et al*., 1994; Girolamo *et al*., 1995). Brefeldin A treatment leads to a ribosylation of BARS and inactivates it. Recently, it has been shown that BARS catalyzes the acylation of lysophosphatidic acid to phosphatidic acid, and that this reaction is essential for membrane fission and thereby Golgi dynamics (Weigert *et al*., 1999). Although initially identified by their different biochemical properties, CtBPs and BARS share a high degree of sequence identity, and the findings that BARS can bind to the same transcription factors as CtBPS and that CtBPs are subject to the brefeldin A-dependent ADP ribosylation indicate that CtBPs and BARS can be considered homolog proteins (Spanfo *et al*., 1999).

The *AN* gene is highly conserved in plants. In DDBJ/EMBL/GenBank searches, EST fragments were found from various plant species that show high sequence identity. Within the completed genome sequence of *Arabidopsis*, no additional genes encoding CtBP/BARS homologs were identified, suggesting that AN represents the plant ortholog of CtBP/BARS.

Table II. Genetic interaction between *AN* and *ZWI*

Cross	No. of trichome branch points					Total
	0[a]	1[a]	2[a]	3[a]	4[a]	
F_1 RLD *zwi-w2* × RLD *an-EM6* #1[b]			43.5 ± 13.1	50.8 ± 13.3	5.6 ± 2.8	636
F_1 RLD *zwi-w2* × RLD *an-EM6* #2[b]			43.4 ± 6.8	54.1 ± 6.7	2.5 ± 1.9	631
F_1 RLD *zwi-w2* × Ler an-X1		1.3 ± 2.0	91.6 ± 4.5	6.0 ± 3.3	1.1 ± 2.7	328
F_1 Col *zwi-3* × RLD *an-EM6*			80.6 ± 4.8	18.4 ± 4.4	1.0 ± 0.7	467
F_1 Col *zwi-3* × L*er an-X1*			94.3 ± 2.7	5.7 ± 2.7		393
F_1 Col *zwi-3* × L*er an-EM4* #1[b]		0.1 ± 0.4	92.0 ± 4.1	7.9 ± 4.2		456
F_1 Col *zwi-3* × L*er an-EM4* #2[b]			93.2 ± 5.1	6.7 ± 5.1		473
F_1 RLD *zwi-9311-11* × L*er an-X1*		1.1 ± 1.2	95 ± 1.6	3.9 ± 2.6		451
F_1 RLD wt × *an-EM6*		0.2 ± 0.3	85.7 ± 2.0	14.0 ± 2.1		1176
F_1 Col wt × RLD *an-EM6*			87.1 ± 1.8	12.9 ± 1.8		335
F_1 Ler_D × RLD *an-EM6*			92.1 ± 3.2	7.9 ± 3.2		319
F_1 Col wt × Ler *an-EM4*			98.7 ± 2.0	1.3 ± 2.0		297
F_1 RLD wt × L*er an-X1*			80.6 ± 3.8	19.4 ± 3.8		449
F_1 Col wt × L*er an-X1*			99.6 ± 1.3	0.4 ± 1.3		408
F_1 Ler_{USA} × RLD *zwi-w2*		0.7 ± 1.6	78.4 ± 5.3	20.9 ± 5.3		277
F_1 Ler_D × Col *zwi-3*			94.5 ± 1.9	5.6 ± 1.9		392
RLD wt #1		0.5 ± 0.9	77.4 ± 16.4	22.1 ± 16.4		767
RLD wt #2		0.3 ± 0.5	69.7 ± 6.7	30.0 ± 6.6		1361
Ler_D			62.5 ± 9.6	37.5 ± 9.6		467
Ler_{USA}			81.5 ± 5.4	18.5 ± 5.4		386
Col wt			91.8 ± 2.0	8.2 ± 2.0		639
Col *zwi-3*	8.2 ± 3.0	91.9 ± 3.0				558
RLD an-EM6	14.0 ± 8.7	84.9 ± 7.9	1.0 ± 2.1			600
RLD zwi-w2	8.1 ± 2.7	75.1 ± 8.6	15.9 ± 6.3	0.9 ± 0.5		905

[a]Percentage and standard deviation.
[b]Data from two independent crosses are shown.

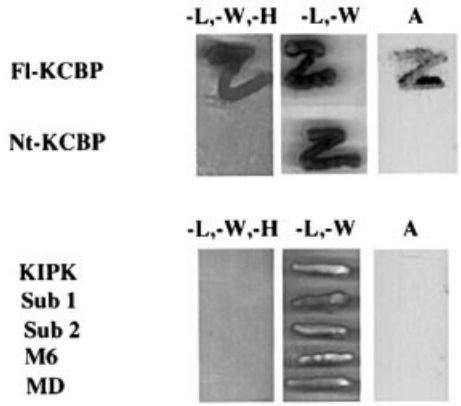

Fig. 6. Two-hybrid interaction between AN and ZWI. Top: yeast strain Y190 (–L/–W/–H) was transformed with full-length KCBP (Fl-KCBP) or Nt-KCBP in pAS1CYH2 and then transformed with AN in pACT2. Colonies were streaked on –L/–W/–H media or –L/–W media and assayed for β-galactosidase activity (A). Bottom: the yeast strain Y190 was also double-transformed with AN in pAS1CYH2 and KIPK, the non-catalytic subclone of KIPK (Sub1), the catalytic domain of KIPK (Sub 2), a KCBP-interacting putative calcium-binding protein (M6) or the motor domain of KCBP (MD) in pACT2 plasmids. The transformants were streaked on –L/–W/–H or –L/–W media. A β-galactosidase assay was performed for a replicate of each transformant (A).

Does AN link vesicle transport to microtubule-based directional transport processes?

A presumed role for AN in the control of Golgi dynamics and vesicle trafficking is in principle consistent with its role in cell morphogenesis. However, it remains unclear why mutations in the *AN* gene specifically affect cell polarity rather than general morphogenesis. A potential explanation is provided by the finding that AN is involved in the organization of the microtubule cytoskeleton. This is supported by two lines of evidence. First, microtubule density is altered in a region-specific manner in *an* mutant trichomes. Secondly, genetic and molecular interactions of AN were found with ZWI/KCBP. *ZWI* is also involved in trichome branching and *zwi* mutants show a phenotype similar to *an* mutants (Hülskamp *et al*., 1994; Folkers *et al*., 1997; Oppenheimer *et al*., 1997). *ZWI* encodes a kinesin motor molecule and was shown to move as a minus end-directed motor molecule on microtubules (Song *et al*., 1997).

It is therefore conceivable that *AN* is required to link Golgi-derived vesicle trafficking with directional transport processes as controlled by the microtubule cytoskeleton or, more specifically, certain motor molecules.

Materials and methods

Plant material and genetic analysis

Plants were grown at constant illumination at 23°C. The wild-type strains used in this work were L*er*, Nd and Columbia-0 (Col). New *an* alleles were isolated from the F_2 progeny of plants mutagenized with EMS. All alleles were induced in a L*er* ecotype background, except for the *an-EM6* allele, which is in a RLD ecotype background. *Agrobacterium*-mediated transformation of *Arabidopsis* plants was performed as described by Clough and Bent (1998).

Molecular analysis of the AN gene

The YAC, BAC and P1 libaries used to establish a chromosomal walk were obtained from the *Arabidopsis* Biological Resources Centre in Ohio.

For further fine mapping, new CAPS markers were generated by the following strategy: BACs were shotgun-subcloned into pBluescriptKS+

(Stratagene), inserts of appropriate size were sequenced, and primers for genomic amplification were designed with the McVector 4.5 software (Kodak Scientific Imaging Systems, New Haven, CT). PCR products were tested for ecotype-specific restriction enzyme polymorphisms. New molecular markers established the following differences between L*er* and Nd: T2,5, GGTGCCAAATTAGAGTTTCAGGGG and TTGTGGAGC-AGATATTGCGTGC shows a length polymorphism, 2.9 kb in L*er* and 2.8 kb in Nd; postZat, TGCTGACTTCCCGCATCGTATG and CGT-CAAAAAGCAAAAAACCGCC shows a *NLA*III polymorphism, 600 bp in L*er* and 580 bp in Nd; M-left, AGCATCAACCTGTAAAGAAGG-ATAATC and TTCGTCAATGTAGTTTTGCTCC shows a *Bsu*1365I polymorphism, 210 bp in L*er* and 195 bp in Nd; K8-2, AATGAAATA-TAATGGTCGTGTGG and AACCACCATCCTCAAAGGCTC shows a *Tru*1I polymorphism, 240 bp in L*er* and 230 bp in Nd; ATHACS, AGAAGTTTAGACAGGTAC and AAATGTGCAATTGCCTTC shows length polymorphism, 256 bp in L*er* and 259 bp in Nd; and T2P5, TGGTAGACGATAGTGACAGGTGGA and GGATTGGCTTAAAT-CAATGGTGGG shows a *Tru*1 polymorphism, 160 bp in L*er* and 145 bp in Nd.

For the genomic rescue of *an* mutants, a 4186 bp long genomic *Spe*I–*Hin*dIII fragment was cloned in pBluescriptKS and subcloned as a *Sac*I–*Cfr*91 fragment into pBAR A. The *35S:AN* construct was obtained by PCR amplification of a cDNA by RT–PCR using primers introducing a *Bam*HI site on both ends and cloning it directly into *pAR19*. To construct the *35S:GFP4:AN* fusion, the *AN* coding region was PCR amplified, introducing a *Acc*65I site and a *Bam*HI site, and GFP4 was PCR amplified, introducing a *Cfr*9I and a *Bam*HI site. The two fragments were cloned into the *Cfr*9I and *Bam*HI sites of pBluescriptKS, and further subcloned into pBAR35S using *Cfr*9I and *Bam*HI. The *AN:GUS* construct was obtained by PCR amplification of the complete non-coding region between the *AN* gene and the neighboring gene, introducing a *Hin*dIII and a *Sal*I site. This fragment was cloned into *pGUS1* (Peleman, 1989). The *GL2:GFP:MAP4* construct was created by cloning the *Nco*I–*Not*I *GFP:MAP4*-fusion fragment into pBluescriptKS, introducing a *Pst*I site by using the corresponding linker. Subsequently, the fragment was subcloned as a *Cfr*9I–*Sac*I fragment into *pBI101* containing the *GL2* promoter (Szymanski *et al*., 1998).

For semi-quantitative RT–PCR, we used different cycle numbers to ensure that amplifications were within the linear range for each primer pair. *AN* was amplified with 35 cycles using the following primers: DHMYBB, 5′-TGCAGATTACAGTGAGGAAGTATGG; and DHF4, 5′-CGACATTCGTCCAGAGAACC. As a control, we amplified the translation elongation factor EF1 with 25 cycles using the following primers (Liboz *et al*., 1990): EF1A4-RP, 5′-TTGGCGGCACCCT-TAGCTGGATCA; and EF1A4-UP, 5′-ATGCCCCAGGACATCGTGA-TTTCAT.

Sequence analysis

Sequence comparisons were made by BLAST (Altschul *et al*., 1990) and BEAUTY searches (Whorley *et al*., 1995). Sequence alignment was performed with the multiple sequence alignment program at the BCM Search Launcher (http://dot.imgen.bcm.tmc.edu:9331/multi-align/) and BOXSHADE version 3.21 by K.Hoffmann and M.Baron at EmbNet (http://www.ch.embnet.org/software/).

Yeast two-hybrid analysis

AN cDNA was cloned as a *Bam*HI fragment into pACT2 and pAS1CYH2. The N-terminal KCBP plasmid was constructed by cloning a *Sac*I–*Not*I fragment (amino acids 12–1261) of *Arabidopsis* KCBP into pET32b. This plasmid was then cut with *Nco*I, releasing a 2.8 kb fragment (amino acids 12–924), which was ligated into pAS1CYH2 digested with *Nco*I. KIPK/pACT2 was isolated in a two-hybrid screen with Nt-KCBP (Day *et al*., 2000). Subclones of KIPK were made using PCR-generated fragments. Primers were designed to amplify an N-terminal fragment from amino acids 1–347 and a C-terminal fragment from amino acids 323–744. A *Bam*HI site was included in the 5′ primers and a *Xho*I site in the 3′ primers. Primers used were: KIPK1S, 5′-CGGGATCCGATGCCTGTAAACGA-TAAACC-3′; KIPK1A, 5′-CCGCTCGAGAGTGTCGTAAACCCAA-AGAGCC-3′; KIPK2S, 5′-CGGGATCCCATGTCGATGGATGTA-GATGGG-3′; and KIPK2A, 5′-CCGCTCGAGACTCAAGATGATC-GCCTATGGC-3′. pET32b and the PCR-generated fragments were cut with *Bam*HI and *Xho*I, ligated and used to transform *Escherichia coli* (BL21). Subclones were cut from pET32b using *Nco*I and *Xho*I, and ligated into *Nco*I–*Xho*I-cut pACT2. All clones were sequenced to confirm the accuracy of the PCR product and in-frame ligation. M6 is a putative calcium-binding protein that interacts with the motor domain of KCBP (T.R.Thomas, I.Day and A.R.Reddy, manuscript in preparation). A motor domain subclone of KCBP was constructed by PCR amplification of a C-terminal fragment coding for amino acids 860–1261, including the motor domain, calmodulin-binding domain and a small portion of the coiled-coil region. The primers included a site for *Bsp*HI, which, when cut, has ends compatible with *Nco*I. pAS1CYH2 was digested with *Nco*I and the fragment with *Bsp*HI; they were ligated and used to transform *E.coli* (DH5a).

Two-hybrid interactions were analyzed as described previously (Day *et al*., 2000).

Cytological methods and images

For particle bombardment, gold particles (1 μm; Bio-Rad, Hercules, CA) were coated with AN–GFP DNA following the manufacturer's directions. Particles were delivered into onion epidermal cells using a Biolistic PDS-1000/He system (Bio-Rad) with 1100 p.s.i. rupture discs under a vacuum of 62.5 mm Hg. After bombardment, the onion slices were maintained on moist filter paper in parafilm-sealed plastic Petri dishes. Epidermal peels were mounted in tap water and observed from 24 to 72 h after bombardment.

Confocal laser-scanning microscopy was carried out using the TCS-NT program (Leica, Bensheim, Germany). To determine the relative density of microtubules between the tip region and the basal region of trichomes, the ratio of pixel densities of equally sized areas was determined for each trichome using the program Metamorph 4.5r4 (Adobe, Mountain View, CA). Whole-mount GUS stainings were performed as described previously (Sessions, 1999). Images were processed with Aldus Freehand 7.0 (Aldus Corp., Seattle, WA) and Adobe Photoshop 3.0 software.

Acknowledgements

We thank members of the authors' laboratory for critically reading the manuscript. We would like to thank M.Koornneef for making available the *an–cer1* double mutant. This work was supported by the Volkswagen Stiftung to M.H., a DFG grant to M.H. and a Boehringer-Ingelheim-Fonds fellowship to U.F.

References

Altschul,S.F., Gish,W., Miller,W., Myers,E.W. and Lipman,D.J. (1990) Basic local alignment search tool. *J. Mol. Biol.*, **215**, 403–410.

Asryants,R., Kuzminskaya,E., Tishkov,V., Douzhenkova,I. and Nagradova,N. (1989) An examination of the role of arginine residues in the functioning of D-glyceraldehyde-3-phosphate dehydrogenase. *Biochim. Biophys. Acta*, **997**, 159–166.

Bernard,N. *et al*. (1997) D-2-hydroxy-4-methylvalerate dehydrogenase from *Lactobacillus delbrueckii* subsp. *bulgaricus*. II. Mutagenic analysis of catalytically important residues. *Eur. J. Biochem.*, **244**, 213–219.

Clough,S. and Bent,A. (1998) Floral dip: a simplified method for *Agrobacterium*-mediated transformation of *Arabidopsis thaliana*. *Plant J.*, **16**, 735–743.

Day,I.S., Miller,C., Golovkin,M. and Reddy,A.R. (2000) Interaction of a kinesin-like calmodulin-binding protein with a protein kinase. *J. Biol. Chem.*, **275**, 13737–13745.

Durfee,T., Becherer,K., Chen,P.L., Yeh,S., Yang,Y., Kilburn,A.E., Lee,W.H. and Elledge,S.J. (1993) The retinoblastoma protein associates with the protein phosphatase type 1 catalytic subunit. *Genes Dev.*, **7**, 555–569.

Folkers,U., Berger,J. and Hülskamp,M. (1997) Cell morphogenesis of trichomes in *Arabidopsis*: differential regulation of primary and secondary branching by branch initiation regulators and cell size. *Development*, **124**, 3779–3786.

Girolamo,M.D., Silletta,M.G., Matteis,M.A.D., Braca,A., Colanzi,A., Pawlak,D., Rasenick,M.M., Luini,A. and Corda,D. (1995) Evidence that the 50 kDa substrate of brefeldin A-dependent ADP-ribosylation binds GTP and is modulated by the G-protein βγ subunit complex. *Proc. Natl Acad. Sci. USA*, **92**, 7065–7069.

Hülskamp,M. (2000) How plants split hairs. *Curr. Biol.*, **10**, R308–R310.

Hülskamp,M., Misera,S. and Jürgens,G. (1994) Genetic dissection of trichome cell development in *Arabidopsis*. *Cell*, **76**, 555–566.

Hülskamp,M., Folkers,U. and Schnittger,A. (1999) Trichome development in *Arabidopsis thaliana*. *Int. Rev. Cytol.*, **186**, 147–178.

Koornneef,M., Dellaert,L.W.M. and van der Veen,J.H. (1982) EMS- and

radiation-induced mutation frequencies at individual loci in *Arabidopsis thaliana*. *Mutat. Res.*, **93**, 109–123.
Krishnakumar,S. and Oppenheimer,D.G. (1999) Extragenic suppressors of the *Arabidopsis zwi-3* mutation identify new genes that function in trichome branch formation and pollen tube growth. *Development*, **126**, 3079–3088.
Liboz,T., Bardet,C., Thai,A.L.V., Axelos,M. and Lescure,B. (1990) The four members of the gene family encoding the *Arabidopsis thaliana* translation elongation factor EF-1α are actively transcribed. *Plant Mol. Biol.*, **14**, 107–110.
Lippincott-Schwartz,J., Yuan,L.C., Bonifacino,J.S. and Klausner,R.D. (1989) Rapid redistribution of Golgi proteins into the ER in cells treated with brefeldin A: evidence for membrane cycling from Golgi to ER. *Cell*, **56**, 801–813.
Luo,D. and Oppenheimer,D.G. (1999) Genetic control of trichome branch number in *Arabidopsis*: the roles of the *FURCA* loci. *Development*, **126**, 5547–5557.
Marks,M.D. (1997) Molecular genetic analysis of trichome development in *Arabidopsis*. *Annu. Rev. Plant Physiol. Plant Mol. Biol.*, **48**, 137–163.
Mathur,J. and Chua,N.H. (2000) Microtubule stabilization leads to growth reorientation in *Arabidopsis thaliana* trichomes. *Plant Cell*, **12**, 465–477.
Mathur,J., Spielhofer,P., Kost,B. and Chua,N.-H. (1999) The actin cytoskeleton is required to elaborate and maintain spatial patterning during trichome cell morphogenesis in *Arabidopsis thaliana*. *Development*, **126**, 5559–5568.
Matteis,M.D. *et al*. (1994) Stimulation of endogenous ADP-ribosylation by brefeldin A. *Proc. Natl Acad. Sci. USA*, **91**, 1114–1118.
Nibu,Y., Zhang,H. and Levine,M. (1998) Interaction of a short-range repressors with *Drosophila* CtBP in the embryo. *Science*, **280**, 101–104.
Oppenheimer,D.G. (1998) Genetics of plant cell shape. *Curr. Opin. Plant Biol.*, **1**, 520–524.
Oppenheimer,D.G., Pollock,M.A., Vacik,J., Szymanski,D.B., Ericson,B., Feldmann,K. and Marks,M.D. (1997) Essential role of a kinesin-like protein in *Arabidopsis* trichome morphogenesis. *Proc. Natl Acad. Sci. USA*, **94**, 6261–6266.
Peleman,J., Boerjan,W., Engler,G., Seurinck,J., Botterman,J., Alliote,T., Van Montagu,M. and Inze,D. (1989) Strong cellular preference in the expression of a housekeeping gene of *Arabidopsis thaliana* encoding S-adenosylmethionine synthase. *Plant Cell*, **1**, 81–93.
Perazza,D., Herzog,M., Hülskamp,M., Brown,S., Dorne,A. and Bonneville,J. (1999) Trichome cell growth in *Arabidopsis thaliana* can be depressed by mutations in at least five genes. *Genetics*, **152**, 461–476.
Reddy,A.S., Narasimhulu,S.B., Safadi,F. and Golovkin,M. (1996a) A plant kinesin heavy chain-like protein is a calmodulin-binding protein. *Plant J.*, **10**, 9–21.
Reddy,A.S., Safadi,F., Narasimhulu,S.B., Golovkin,M. and Hu,X. (1996b) A novel plant calmodulin-binding protein with a kinesin heavy chain motor domain. *J. Biol. Chem.*, **271**, 7052–7060.
Redei,G.P. (1962) Single locus heterosis. *Z. Vererbungsl.*, **93**, 164–170.
Schaeper,U., Subramanian,T., Lim,L., Boyd,J. and Chinnadurai,G. (1998) Interaction between a cellular protein that binds to the C-terminal region of adenovirus E1A (CtBP) and a novel cellular protein is disrupted by E1A through a conserved PLDLS motif. *J. Biol. Chem.*, **273**, 8549–8552.
Sessions,A., Weigel,D. and Yanofsky,M. (1999) The *Arabidopsis thaliana* MERISTEM LAYER 1 promotor species epidermal expression in meristems and young primordia. *Plant J.*, **20**, 259–263.
Song,H., Golovkin,M., Reddy,A.S. and Endow,S.A. (1997) *In vitro* motility of AtKCBP, a calmodulin-binding kinesin protein of *Arabidopsis*. *Proc. Natl Acad. Sci. USA*, **94**, 322–327.
Spanfo,S. *et al*. (1999) Molecular cloning and functional characterization of brefeldin A-ADP-ribosylated substrate. A novel protein involved in the maintenance of the Golgi structure. *J. Biol. Chem.*, **274**, 17705–17710.
Stoll,V., Kimber,M. and Pai,E. (1996) Insights into substrate binding by D-2-ketoacid dehydrogenases from the structure of *Lactobacillus pantosus* D-lactate dehydrogenase. *Structure*, **4**, 437–447.
Szymanski,D.B., Jilk,R.A., Pollock,S.M. and Marks,M.D. (1998) Control of GL2 expression in *Arabidopsis* leaves and trichomes. *Development*, **125**, 1161–1171.
Szymanski,D.B., Marks,M.D. and Wick,S.M. (1999) Organized F-actin is essential for normal trichome morphogenesis in *Arabidopsis*. *Plant Cell*, **11**, 2331–2348.
Torres-Ruiz,R.A. and Jürgens,G. (1994) Mutations in the *FASS* gene uncouple pattern formation and morphogenesis in *Arabidopsis* development. *Development*, **120**, 2967–2978.
Traas,J., Bellini,C., Nacry,P., Kronenberger,J., Bouchez,D. and Caboche,M. (1995) Normal differentiation patterns in plants lacking microtubular preprophase bands. *Nature*, **375**, 676–677.
Tsuge,T., Tsukaya,H. and Uchimiya,H. (1996) Two independent and polarized processes of cell elongation regulate leaf blade expansion in *Arabidopsis thaliana*. *Development*, **122**, 1589–1600.
Tsukaya,H. (1995) Developmental genetics of leaf morphogenesis in dicotyledonous plants. *J. Plant Res.*, **108**, 407–416.
Tsukaya,H., Tsuge,T. and Uchimiya,H. (1994) The cotyledon: a superior system for studies of leaf development. *Planta*, **195**, 309–312.
Weigert,R. *et al*. (1999) CtBP/BARS induces fission of Golgi membranes by acylating lysophosphatidic acid. *Nature*, **402**, 429–433.
Whorley,K., Wiese,B. and Smith,R. (1995) BEAUTY: an enhanced BLAST-based search tool that integrates multiple biological information resources into sequence similarity search results. *Genome Res.*, **5**, 173–184.

Received August 29, 2001; revised and accepted January 30, 2002